

Magnetic field asymmetry of nonlinear transport in carbon nanotubes

J. Wei, M. Shimogawa, Z. Wang, I. Radu, R. Dormaier, and D.H. Cobden

We demonstrate that nonlinear transport through a two-terminal mesoscopic sample is not symmetric in magnetic field B . More specifically, we have measured the lowest order B -asymmetric terms in single-walled carbon nanotubes. Theoretically, the size of these terms can be used to infer both the strength of electron-electron interactions and the handedness of the nanotube. Consistent with theory, we find that at high temperatures the B -linear term is small and has a constant sign independent of Fermi energy, while at low temperatures it develops mesoscopic fluctuations. We also find significant magnetoresistance of nanotubes in the metallic regime which is currently unexplained.

The conductance G of a two-terminal sample in linear response must be an even function of applied magnetic field \mathbf{B} , that is, $G(B) = G(-B)$ [1,2]. The underlying principle that leads to this Onsager symmetry is the time-reversal symmetry of the equilibrium microscopic dynamics, combined with the fact that \mathbf{B} changes sign on time reversal. There is no such strong symmetry requirement for nonlinear response. Nevertheless, some useful observations may also be made about the nonlinear transport coefficients. These are most readily framed by expanding the current I in powers of the voltage V :

$$I = G(B)V + \chi(B)V^2 + \dots, \quad (1)$$

and focusing on the first nonlinear coefficient χ , which we expand in powers of B :

$$\chi(B) = \chi_0 + \alpha B + \dots \quad (2)$$

One observation is that for a sample with helical symmetry the sign of the coefficient α in Eq. 2 depends on the handedness [3]. This is essentially because the axial vector \mathbf{B} combined with the helicity defines a direction which is inverted if \mathbf{B} is inverted, in the same way that the direction of motion of a screw depends on the sense in which it is rotated. This could for example in principle allow one to distinguish between left- and right-handed chiral carbon nanotubes having otherwise identical structure.

A second observation is that the magnitude of α is proportional to the strength of electron-electron (e-e) interactions in the sample. This has been shown to be the case at both high and low temperature T . In the high T limit α can be calculated using a Boltzmann equation approach [4], and it turns out to be proportional to the e-e scattering rate. In this regime, measurements of α have been made on a macroscopic sample [5], but not on any nanoscale samples. In the low T limit [6,7] (the mesoscopic regime) no experiments have been reported. This regime may be considered using diagrammatic calculations [8], or using the Landauer formula [9]. Briefly, according to the Landauer formula the Onsager symmetry is obeyed at each energy. In the absence of interactions the total current is the sum over contributions at all energies, and it is thus also even in B and α is zero. However, the electric field due to the applied voltage V induces local changes in the current and electron densities which contain B -odd components (as for example in the Hall effect). This produces B -odd components in the scattering potential, and thence in the nonlinear transport coefficients, which are proportional to the interaction parameter β . As a result, α can in principle be used to determine the strength of interactions in the system.

It is well known that e-e interactions are important in single-walled carbon nanotubes because of their one-dimensional (1D) electronic dispersion [10]. Describing the conduction electrons in an infinite clean nanotube as a Luttinger liquid [11,12] allows one to explain the power-law energy dependences of tunneling rates seen in several transport experiments [13,14]. However, real nanotubes are finite and disordered, and the nature of transport in them at high and low temperatures remains an open question. For this reason, we have chosen single-walled nanotubes as a test system in which to carry out the first specific and detailed measurements of nonlinear coefficients χ and α . We exploit the fact that in a single-walled nanotube, unlike a pure 1D system, there is a simple mechanism for generating magnetotransport effects: the band structure is modified by application of a magnetic field along the tube axis due to the Aharonov-Bohm phase [15,4]. Our results are in agreement with the general expectations of the theory mentioned above: near room temperature α is small and its sign is independent of gate voltage, while as the temperature is decreased α grows and develops random mesoscopic fluctuations. In addition, we find magnetoresistance in nanotubes in the metallic regime persisting up to room temperature, which is not currently explained. These results may help

to stimulate theoretical work on the basic problems of linear and nonlinear magnetotransport in a 1D electron system.

Each device consists of an individual single-walled carbon nanotube formed by chemical vapor growth from iron catalyst particles [16,17], with two gold contacts, 4 μm apart, patterned by thermal evaporation through a stencil. The substrate is 450 nm of thermal SiO_2 on a highly n-doped silicon wafer, to which a gate voltage V_g is applied through a $10 \text{ M}\Omega$ resistor. An atomic force microscope image of the device (Device 1) on which we focus in this paper is shown in Fig. 1a. The nanotube's diameter is approximately 1.3 nm, and its characteristics indicate that it is metallic. We have also made detailed measurements on a *p*-type semiconducting nanotube device, but a metallic nanotube has two advantages for the present study: first, the effects of e-e interactions are easier to distinguish from band structure effects; and second, the theory of the B -asymmetric terms has so far only been done for metallic conductors.

Since nonlinear measurements are subject to misinterpretation we specify the details of the arrangement used to measure G and χ in Fig. 1a. A sinusoidal bias of rms amplitude V_0 at frequency f (typically 650 Hz) is applied to one contact with the other connected to a virtual-ground current preamplifier (Ithaco 1211). A $10 \mu\text{F}$ capacitor in series enforces zero dc current. The rms harmonic current components I_f and I_{2f} are extracted from the amplifier output using lockin amplifiers. In all the measurements V_0 is kept sufficiently small ($V_0 \approx kT/e$) to ensure that $I_{2f} \ll I_f$ and that $I_{2f} \propto V_0^2$, so that harmonics beyond I_{2f} are negligible. The first two coefficients in Eq. (1) can then be obtained as $G = I_f/V_0$ and $\chi = 2I_{2f}/V_0^2$.

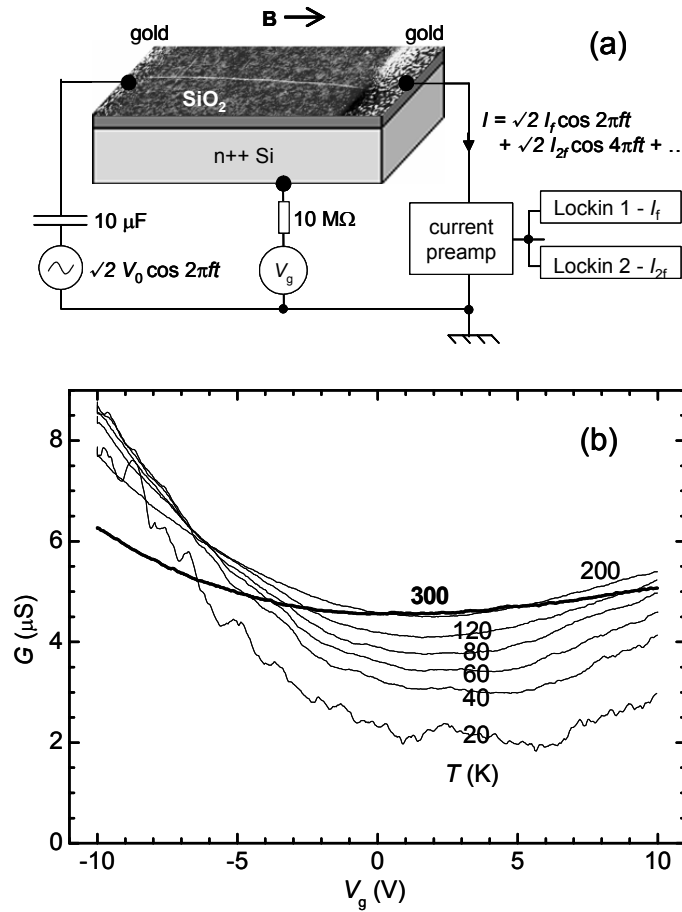


Fig 1. (a) Tapping-mode atomic force microscope image of Device 1 combined with a schematic diagram of the measurement setup. The separation of the gold contacts is 4 μm . The orientation of the magnetic field parallel to the nanotube is indicated. (b) Linear conductance vs gate voltage at a series of temperatures.

The behavior of the linear conductance of Device 1 at zero magnetic field is illustrated in Fig. 1b. The weak dependence on V_g at room temperature (bold trace) is characteristic of a metallic (or a small-gap) nanotube. As T is decreased from 300 K, G initially rises and then falls towards zero at liquid helium temperatures. The temperature at which G is maximum varies between about 250 K for $V_g = 2 \text{ V}$ and 40 K

for $V_g = -10$ V. For $T < 20$ K, a dense ‘grass’ of aperiodic and unreproducible Coulomb oscillations appears (not shown), and by 4.2 K G is unmeasurably small.

That dG/dT is negative at room temperature indicates that the resistance is dominated by the bulk resistance of the nanotube, which increases as T increases due to phonon scattering. Poor contacts would instead make dG/dT positive [13]. Assuming the resistance is distributed along the nanotube, in the incoherent limit it can be characterised by a backscattering length l_b given by $G_{max}/G = 1 + L/l_b$ [9]. Here $G_{max} = 4e^2/h = 155$ μ S is the conductance in the absence of backscattering and $L = 4$ μ m is the nanotube length. At 300 K we have $G \sim 5$ μ S, giving $l_b \sim 150$ nm. This is shorter than the phonon scattering length, which is 1 to 2 μ m [18], implying that backscattering is predominantly due to disorder. This is consistent with the behavior in the low T regime where we infer from the details of the Coulomb oscillations that the disorder causes the nanotube to break up electrically into a series of submicron regions [19] whose typical charging energy is several meV and whose self-capacitance is dominated by capacitance to the gate. We do not know the precise origin of this disorder, which is much higher than in the cleanest nanotube devices [18]. It may be explained by a high density of contaminants on the substrate as well as on the nanotube surface.

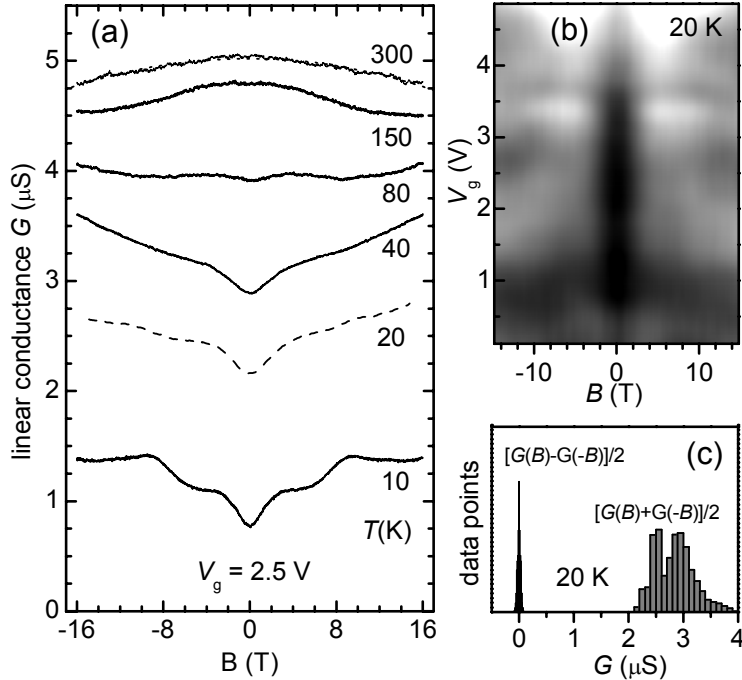


Fig. 2. (a) Linear conductance G vs. magnetic field B at a series of temperatures for a fixed gate voltage, measured using the setup in Fig. 1. (b) Grayscale plot of $G(V_g, B)$ at $T = 20$ K. Black is 2.2μ S, white is 3.5μ S. (c) Histogram of B -symmetrized and B -antisymmetrized parts of G , averaged over all V_g and B , from the dataset in (b).

We turn now to the effects of magnetic field, considering first the linear conductance G . The variation of G with B and T is illustrated in Fig. 2a. At $T = 300$ K the magnetoconductance is negative and approximately quadratic up to 16 T. Fitting it to $G(B) = G_0(1 + \gamma B^2)$ at each gate voltage we find that the parameter γ varies steadily from approximately -2×10^{-4} T $^{-2}$ at $V_g = 0$ to -4×10^{-4} T $^{-2}$ at $V_g = 5$ V. In the semiconducting device at 200 K we found γ was positive, reaching a peak of $+4 \times 10^{-3}$ T $^{-2}$ close to threshold but maintaining a value of $+2 \times 10^{-4}$ T $^{-2}$ in the metallic regime. Indeed, a positive magnetoconductance near threshold in a semiconducting nanotube is the expected result of the decreasing bandgap induced by the Aharonov-Bohm flux [4,15,20,21]. However, to our knowledge no mechanism has been put forward to date which can explain negative magnetoconductance, or the presence of significant magnetoconductance in the metallic regime [22].

As the temperature decreases, G develops nonperiodic oscillations as a function both of V_g (see Fig. 1b) and of B (see Fig. 2a). Fig. 2b is a greyscale plot of $G(V_g, B)$ at 20 K. Let us compare these oscillations with the predictions of a single-particle model of quantum interference [21,23] in the presence of multiple scatterers, taking into account the diamagnetic shifts of the bands [15,20]. In this model, we estimate a characteristic oscillation period in magnetic field $B_c \sim 4(h/e)/(L_{eff}d)$, determined by finding the magnetic flux

required to shift the relative phase difference between typical electron paths in the K and K' subbands by 2π . Here d is the nanotube diameter and we estimate the effective path length L_{eff} to be the lesser of the nanotube length, $L = 4 \mu\text{m}$, and the thermal length, $L_T \sim h\nu_F/k_B T$. For $T = 20 \text{ K}$ we have $L_T \sim 2 \mu\text{m}$, giving $B_c \sim 6 \text{ T}$. This is compatible with the oscillations seen in Fig. 2a. The model also predicts a gate-voltage period $\sim h\nu_F/(eL_{\text{eff}})$ of a few mV (taking into account the capacitance being dominated by the gate). Such short-period oscillations are not resolved in the measurements presented in Fig. 2b, and are only partially resolved in the 20 K trace in Fig. 1b, so we cannot compare the results quantitatively with this prediction. However, features are visible in Fig. 2b which vary much more slowly with V_g . In particular, there is a dip at $B = 0$ having a half-width of $\sim 2 \text{ T}$ which can be seen $T < 80 \text{ K}$ and which persists over the entire range of V_g . Again, no theory is available to explain such behavior, although it bears a suggestive similarity to the weak localization dip seen in conventional metals as well as multiwalled nanotubes [24] at low temperatures.

Fig. 2c is a histogram of the symmetrized and antisymmetrized parts of $G(B)$ at 20 K, showing that the antisymmetric part is much smaller than the symmetric part. Since the absence of an antisymmetric component is required by Onsager symmetry, we take this as evidence that the measurement is indeed effectively two-terminal. It also demonstrates the reproducibility of the device characteristics. (The visible deviation from symmetry about $B = 0$ in the 20 K (dashed) sweep in Fig. 2a and the broadening of the black peak in Fig. 2c resulted from drift over the two-hour timescale of the magnetic field sweep.)

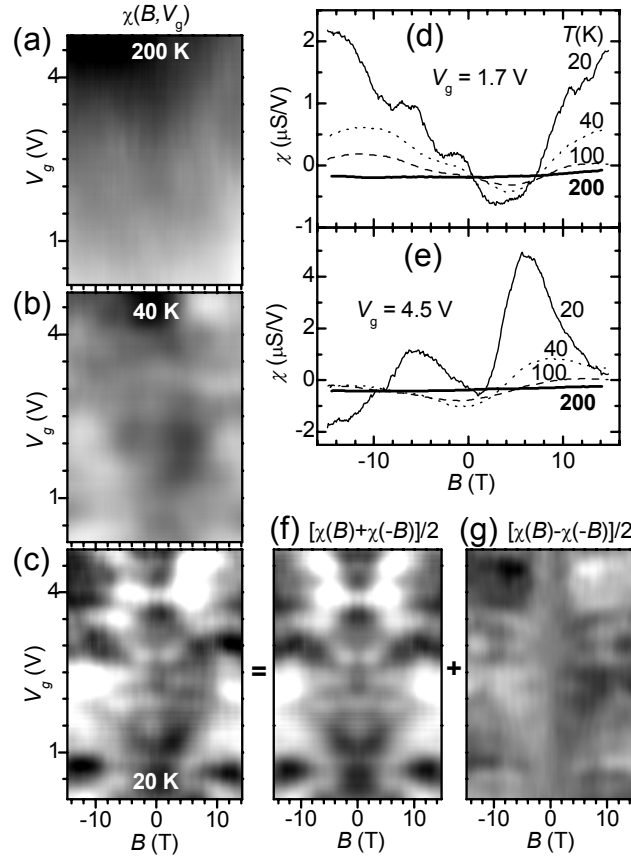


Fig. 3. Dependence of the nonlinear coefficient χ on magnetic field B . (a) to (c), Greyscale plots of $\chi(B, V_g)$ at $T = 200 \text{ K}$, 100 K and 20 K . Black: $-2 \mu\text{S/V}$, white: $+2 \mu\text{S/V}$. (d), (e) Traces of χ vs B at a series of temperatures for $V_g = 1.7 \text{ V}$ and $V_g = 4.5 \text{ V}$. (f) and (g), Greyscale plots of the B -symmetric and B -antisymmetric parts of χ at $T = 20 \text{ K}$.

The variation of the *nonlinear* coefficient χ with B , V_g and T is illustrated in Fig. 3. Figs. 3a-c are greyscale plots of $\chi(V_g, B)$ at three different temperatures. Figs. 3d and 3e show line traces of χ vs B at two selected gate voltages. At the highest temperature of $T = 200 \text{ K}$ (bold traces), χ is small and varies slowly with B up to 16 T. Like G , χ develops oscillations as a function of both V_g and B as the sample is cooled. In contrast with G however, χ is clearly not symmetric about $B = 0$. Figs. 3f and 3g are greyscale plots of the

symmetric and antisymmetric parts of χ at $T = 20$ K. We believe this is first time that B -asymmetric two-terminal transport has been measured reliably and in detail.

We note that the value of χ_0 is determined not only by the intrinsic asymmetry of the device but also by the asymmetry of the measurement (Fig. 1a): applying a bias V_0 to the source generates a nonlinear current due to the change in G caused by the resulting change in average potential difference between the gate and the nanotube, leading to a ‘self-gating’ contribution $I_{2f(\text{self-gating})} \sim (dG/dV_g)V_0^2/4$ [25]. This effect must be purely symmetric in B , as is dG/dV_g , and cannot contribute to the B -antisymmetric part of χ reported above.

To date no predictions specific to nanotubes exist with which we can quantitatively compare these measurements of χ . Nevertheless, the theory mentioned in the introduction leads to qualitative expectations for the behavior of the B -linear coefficient α in Eq. (2). At high T , the sign of α should depend on the handedness of the nanotube and its magnitude is proportional to β^2 [4]. In this regime α should vary slowly, without oscillating, as a function of Fermi energy and thus of V_g . At low T , in the mesoscopic regime, as a result of disorder one expects mesoscopic fluctuations of α characterised by correlation functions [6]. Since the disorder should have no preferred chirality, one expects $\langle \alpha \rangle = 0$, where the average is taken over disorder realizations. For a conventional mesoscopic metallic sample [6] it is predicted that $\langle \alpha^2 \rangle \propto \beta^2/T^2$.

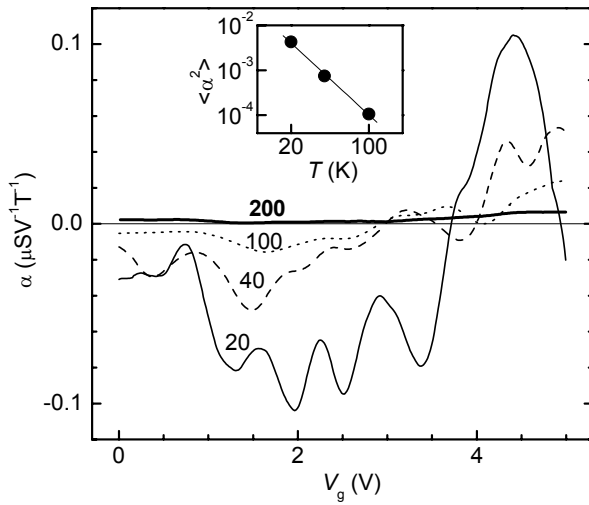


Fig. 4. (a) Variation of the V^2B coefficient α with V_g at a series of temperatures. Inset: log-log plot of $\langle \alpha^2 \rangle$ vs T . The straight line simply indicates a $1/T^2$ dependence.

For comparison with the experiments we extracted values of α by fitting a straight line of the form $\chi_0 + \alpha B$ to the data points of χ vs B in the range -2 T $< B < +2$ T, doing so at each value of V_g and T . The results for α are shown in Fig. 4. At the highest temperature of 200 K, α is small and varies slowly with V_g without changing sign. This is consistent with the above expectations. As T decreases α develops oscillations which cause its sign to alternate as a function of V_g , again consistent with the expectations. In the inset we plot $\langle \alpha^2 \rangle$, obtained by averaging α^2 over V_g , against T . The results are surprisingly consistent with the $1/T^2$ dependence (solid line) mentioned above, in spite of the ostensible inapplicability of the calculation in Ref. [6].

In summary, we have carried out the first experimental study of a new transport coefficient in nanoscale devices, namely, the magnitude α of the V^2B term in the I - V characteristics. We used single-walled carbon nanotubes as a model system. The quantity α provides a way to quantify the role of electron-electron interactions, which is of particular interest in the case of nanotubes. In addition, we find magnetoresistance in the metallic regime at high and low temperatures which acts as a further indication that fundamental aspects of these 1D conductors remain to be understood.

We thank A. Andreev, B. Spivak, O. Vilches and N. Wilson for many useful discussions and J. Chen for providing the catalyst particles. This work was partly supported by the UW Royalty Research Fund, an NSF IGERT fellowship (M.S.), a UW UIF fellowship (I.R.), and a Mary Gates fellowship (R.D.).

References

- [1] L. Onsager, Phys. Rev. 38, 2265 (1931).
- [2] L. Landau and E. M. Lifshitz, *Statistical Physics Volume 1* (Butterworth-Heinemann, 1980).
- [3] B.I. Sturman and V.M. Fridkin, *The Photovoltaic and Photorefractive Effects in Non-centrosymmetric Materials*, (Gordon and Breach, New York, 1992).
- [4] E.L. Ivchenko and B. Spivak, Phys. Rev. B, **66**, 155404 (2002).
- [5] G.L.J.A. Rikken, J. Folling, and P. Wyder, Phys. Rev. Lett. 87, 236602 (2001).
- [6] B. Spivak and A. Zyuzin, Phys. Rev. Lett. 93, 226801 (2004).
- [7] D. Sanchez and M. Buttiker, Phys. Rev. Lett. 93, 106802 (2004).
- [8] A. Larkin and D. Khmelnitskii, JETP **91**, 1815 (1986); V. Falko and D. Khmelnitskii, JETP **68**, 186 (1989).
- [9] S. Datta, *Electronic Transport in Mesoscopic Systems*, (Cambridge University Press, London, 1995).
- [10] D. Mattis, *The Many-Body Problem: An Encyclopedia of Exactly Solved Models in One Dimension* (World Scientific, 1992).
- [11] C. Kane, L. Balents, and M. P. A. Fisher, Phys. Rev. Lett. **79**, 5086 (1997).
- [12] A. Komnik, R. Egger, and A.O. Gogolin, Phys. Rev. B, **56**, 1153 (1997).
- [13] M. Bockrath, D. H. Cobden, J. Lu, A. G. Rinzler, R. E. Smalley, T. Balents, and P. L. McEuen, Nature **397**, 598 (1999).
- [14] Z. Yao, H. W. C. Postma, L. Balents, and C. Dekker, Nature **402**, 273 (1999).
- [15] H. Ajiki and T. Ando, Physica B **201**, 349 (1994).
- [16] J. Kong, A. M. Cassell, H. Dai, Chem. Phys. Lett. 292, 567 (1998).
- [17] Y. Li, J. Liu, Y.Q. Wang, and Z.L. Wang, Chem. Mater. 13, 1008 (2001).
- [18] J.Y. Park, S. Rosenblatt, Y. Yaish, V. Sazonova, H. Ustunel, S. Braig, T. A. Arias, P. Brouwer and P.L. McEuen, Nano Lett, **4**, 517 (2004)
- [19] P. L. McEuen, M. Bockrath, D. H. Cobden, Y.-G. Yoon, and S. G. Louie, Phys. Rev. Lett. **83**, 5098 (1999).
- [20] D. Minot, Y. Yaish, V. Sazonova, and P.L. McEuen, Nature **428**, 536 (2004).
- [21] J. Cao J, Q. Wang, M. Rolandi, and H.J. Dai, Phys. Rev. Lett. **93**, 216803 (2004).
- [22] The contribution of the gold leads to the resistance is negligible.
- [23] W. Liang, M. Bockrath, D. Bozovic, J. Hafner, and M. Tinkham, and H. Park, Nature **411**, 665 (2001).
- [24] A. Bachtold, C. Strunk, J.P. Salvetat, J.-M. Bonard, L. Forro, T. Nussbaumer, and C. Schonenberger, Nature 397, 673 (1999); L. Langer, V. Bayot, E. Grivei, J.-P. Issi, J. P. Heremans, C. H. Olk, L. Stockman, C. Van Haesendonck, and Y. Bruynseraede, Phys. Rev. Lett. 76, 479 (1996); B. Stojet, C. Miko, L. Forro, and C. Strunk; Phys. Rev. Lett. **94**, 186802 (2005).
- [25] A. Lofgren, C.A. Marlow, I. Shorubalko, R.P. Taylor, P. Omling, L. Samuelson, and H. Linke, Phys. Rev. Lett. **92**, 046803 (2004).